Journal of Computer-Aided Molecular Design, 10 (1996) 441–460
ESCOM

J-CAMD 352

A computational study on the relative reactivity of reductively activated 1,4-benzoquinone and its isoelectronic analogs

Yitbarek H. Mariam* and Alesia Sawyer

Department of Chemistry, and Center for Theoretical Studies of Physical Systems, Clark Atlanta University, Atlanta, GA 30314, U.S.A.

Received 5 December 1995
Accepted 15 April 1996

Keywords: *p*-Benzoquinone; *p*-Benzoquinone imine; Redox capacity; Redox cycling; 5-Iminodaunomycin; Anthracyclines; Relative reactivity; Reducibility; Oxidizability

Summary

The redox capacities of *p*-benzoquinone (**I**) and its analogs *p*-benzoquinone imine (**VI**) and *p*-benzoquinone diimine (**XI**) as the simplest model systems for the biochemically important quinone site of the pharmacophores of the anthracyclines has been investigated by AM1 semi-empirical and ab initio methods. The reductive activation of the parent (Q) model systems to their various redox states (quinone radical anion ($Q^{\cdot-}$), semiquinone ($QH^{\cdot}$), semiquinone anion (QH^{-}) and hydroquinone (QH_2)), the internal geometrical reorganization and the redox capacities of the redox states have been examined by using energy-partitioning analysis, reaction enthalpies/energies for electron and proton attachments, adiabatic ionization potentials (IP_{ad}) and electron affinities (EA_{ad}), adiabatic electronegativities (X_{ad}), dipole moments, electrostatic potentials and spin-density surfaces. EA_{ad} data and results of energy-partitioning analysis suggest that the one-electron Q to $Q^{\cdot-}$ reducibility of **VI** is diminished when compared to that of **I**. The data also predict that reduction to $QH^{\cdot}$, QH^{-} and QH_2 is more favorable in **VI** (cf. **I**). Deprotonation enthalpy/energy calculations predict that the oxidizability of the reduced forms of **VI** is diminished when compared to **I**. Overall, the calculations suggest that the redox cycling of **VI** should be diminished if deprotonation is the first step of the autoxidation of the reduced forms. The results suggest that the electron affinity of Q and deprotonation of the reduced forms (e.g., $QH^{\cdot}$) may play important roles in the redox cycling of the anthracyclines. It is further suggested that these same factors are probably responsible for the reduced toxicity of 5-iminodaunomycin, which consists of **VI** as part of its pharmacophore. A comparison of the AM1 results with ab initio results suggests that the AM1 method is capable of predicting trends in redox capacity, nucleophilicity, electrophilicity and electron affinity in the systems investigated.

Introduction

It is widely presumed that the redox chemistry of adriamycin (doxorubicin) and daunomycin (daunorubicin), two of the anthracycline class of antibiotics which are powerful and widely used quinone-containing antitumor drugs [1–5], can generate free radicals during their metabolism [6]. This, and the fact that over ten metabolites have been identified and/or purified from adriamycin alone [7], makes the understanding of the modes of actions and toxities of the anthracyclines very difficult since a good number of these metabolites can be reductively activated forming semiquinones, quinone radical and semiquinone anions, quinone methide radicals [8], etc. After reduction by aerobic or anaerobic pathways, the reduced forms of the drugs can transfer electrons, as has been speculated, to molecular oxygen, forming reactive oxygen species (superoxide anion, hydroperoxide, hydrogen peroxide, etc.) which may be responsible for toxicity in general and for cardiotoxicity in particular. Mechanistically, the generally advanced scheme that is presumed to be compatible with membrane lipid peroxidation and/or DNA damage is [9,10]:

$$Q + e^{-} + H^{+} \rightarrow QH^{\cdot}$$

or

*To whom correspondence should be addressed.

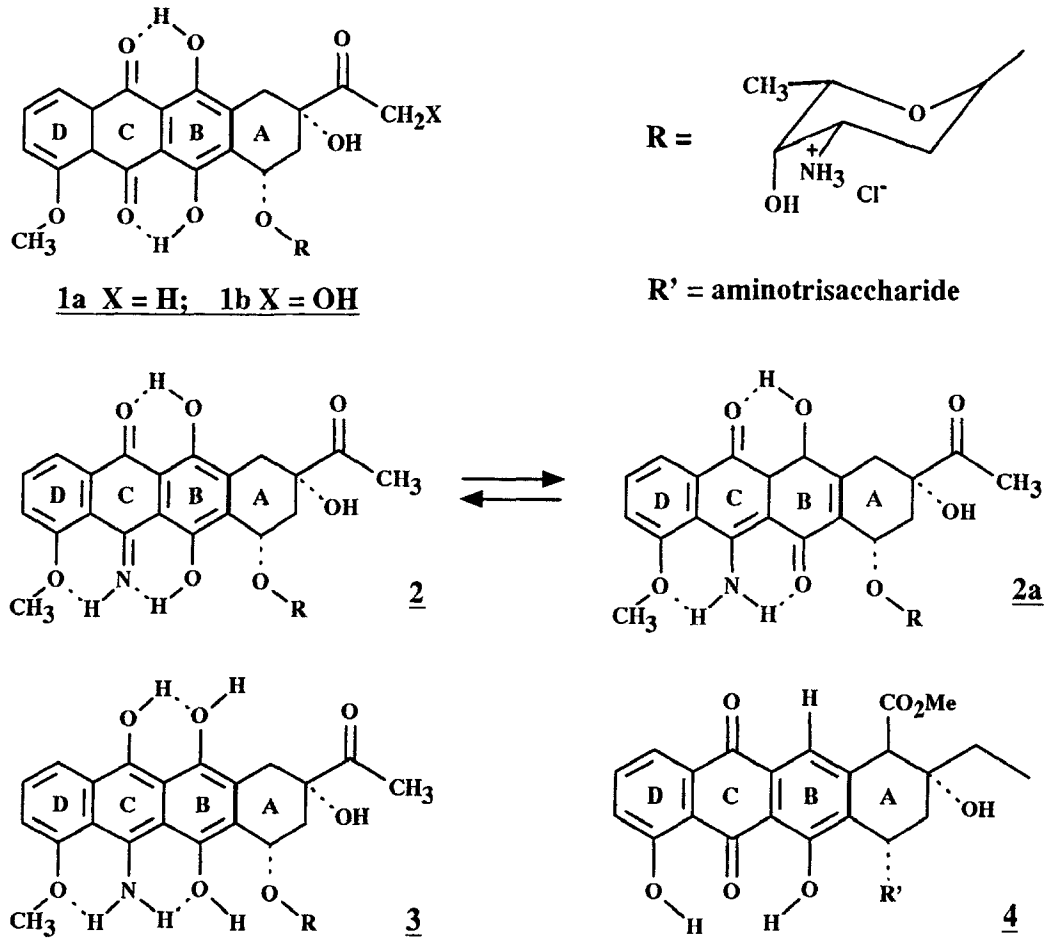

Fig. 1. Structural formulae of daunomycin (**1a**), adriamycin (**1b**), 5-iminodaunomycin (**2**), 5,11-dihydro-5-iminodaunomycin (**3**) and aclacinomycin (**4**).

$$Q + 2e^- + 2H^+ \rightarrow QH_2$$
$$QH_2 + O_2 \rightarrow QH^{\cdot} + HO_2^{\cdot}$$

or

$$QH^{\cdot} + O_2 \rightarrow Q + HO_2^{\cdot}$$
$$HO_2^{\cdot} \rightleftarrows O_2^- + H^+$$

The superoxide anion can, in subsequent steps, undergo the following further reactions:

$$2O_2^- + 2H^+ \rightarrow H_2O_2 + O_2$$
$$H_2O_2 + O_2^- \rightarrow OH^- + OH^{\cdot} + O_2$$

(Haber–Weiss reaction)

$$OH^{\cdot}\ DNA \rightarrow H_2O + DNA^{\cdot}$$

(deoxyribose or base attack)

$$DNA^{\cdot} + O_2 \rightarrow DNA^{\cdot}OO^{\cdot}$$

(strand scission or base decomposition/elimination)

It is generally believed that the dose-related cardiotoxicity of the anthracyclines leading to cardiac lipid peroxidation arises from the same reactive oxygen species.

In the anthracyclines adriamycin and daunomycin (DN) (Fig. 1), it is the presence of the hydroxyquinone functionality that is thought to be responsible for the antitumor activity and the cardiac toxicity [11]. In the case of 5-iminodaunomycin (5IDN) (Fig. 1) in which the biochemically active site has been altered, little or no cardiac toxicity was shown although the drug appeared to show antitumor activity in several commonly used marine tumor models and human tumor xenographs [11]. This chemical activity of 5IDN has been attributed to the markedly diminished capacity of 5IDN to form reactive radical species following the metabolic reduction known to activate both adriamycin and daunomycin [11].

More specifically, the lower cardiotoxicity of 5IDN has been proposed to be its diminished capacity for catalytically producing reactive oxygen species [12]; and, in fact, 5IDN has been described as a redox-incapacitated anthracycline [13]. These conclusions stemmed from the electrochemical results of Lown et al. [12a] which indicated that an aqueous solution of 5IDN was more difficult to reduce than DN and that the reoxidation of 5,11-dihydro-5-iminodaunomycin (3) (Fig. 1) in aqueous solution was much more difficult than the reoxidation of the reduced DN.

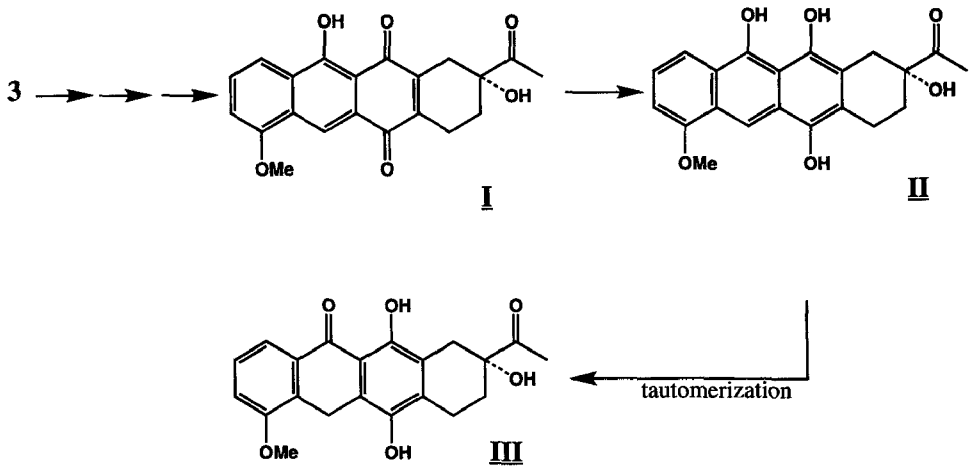

Scheme 1. Reduction of 5,11-dihydro-5-iminodaunomycin (**III**) to the hydroquinone (**II**) of naphthacenedione (**I**).

The issue of 5IDN being a redox-incapacitated anthracycline was, in fact, experimentally investigated by Bird et al. [14], who proposed a possible explanation for the inefficiency of 5IDN to catalyze in vivo the reduction of molecular oxygen to be the facile formation of naphthacenedione (**I**) whose hydroquinone (**II**) tautomerizes to naphthacenone (**III**) (Scheme 1) in preference to reduction of molecular oxygen [14]. The experimental observations raise the question as to what extent the chemical reactivity under consideration should be expected to be different, and as to what exactly might be responsible for this difference. The results of Bird et al. [14], while providing evidence for what takes place in the experimental chemical system that they used, may not be applicable to in vivo or physiological systems and to hydrophobic/non-aqueous media. More importantly, what the reactivity of 5IDN should be, if the facile conversion of 5IDN to naphthacenedione had not occurred, cannot be assessed from the Bird et al. results. In any case, the difference in reactivity arising from such a deceptively minor alteration of the biochemically important quinone site, specifically if it is indeed responsible for the reduced toxicity of 5-iminodaunomycin, has very significant implications from the point of view of the design of anthracyclines with reduced toxicity, and a further understanding of the inherent reactivity is very important.

The thrust of the work in this report is, thus, to compare the relative reactivities of 1,4-benzoquinone (**I**) and 1,4-benzoquinone imine (**VI**) as the simplest model systems for the pharmacophorically important quinone site of the anthracyclines. 1,4-Benzoquinone diimine (**XI**) is also included in this study for the purpose of establishing a trend in reactivity. Within the theoretical framework of the AM1 semiempirical method, the reductive activation of **I**, **VI** and **XI**, the geometrical reorganizations as a result of reductive activation, conformational energy profiles in $QH^{\bullet}$, QH^{-} and QH_2 forms of **I**, **VI** and **XI** as well as the reducibility and oxidizability of the redox states of **I**, **VI** and **XI** have been assessed. The AM1 results predict that the redox cycling of **VI** is less favored, in agreement with the experimental observation that 5IDN is difficult to reduce and the capacity of the reduced form to autoxidize is diminished. It is important to emphasize here that the AM1 results are used to establish trends in reactivity only in relative and qualitative terms, and not for quantitative purposes. In order to put the conclusions gleaned from the AM1 results on firmer ground, the results from ab initio calculations are also presented. The agreement observed between the AM1 and the ab initio results suggests that the AM1 method should be quite useful in investigating the redox capacity of larger systems.

Computational approaches

The quinone (Q) moieties of the drugs can be reductively activated to hydroquinone (QH_2) incorporating two electrons and two protons: $Q + 2e^- + 2H^+ \rightarrow QH_2$. This reaction can be envisioned to occur in four steps: two proton and two electron attachments. One possible sequence of steps for this reaction is shown in Scheme 2, where $Q^{\bullet-}$, $QH^{\bullet}$, QH^- and QH_2 denote the corresponding quinone radical anions, semiquinones, semiquinone anions and hydroquinones of **I**, **VI** and **XI**, respectively. Other less likely routes can also be considered and are briefly discussed in the Results section.

The structures, energies and energetic properties of **I**, **VI** and **XI** and of the various species in Scheme 2

$$\underset{\mathbf{1}}{Q} \xrightarrow{+e^-} \underset{\mathbf{2}}{Q^{\bullet-}} \xrightarrow{+H^+} \underset{\mathbf{3}}{QH^{\bullet}} \xrightarrow{+e^-} \underset{\mathbf{4}}{QH^-} \xrightarrow{+H^+} \underset{\mathbf{5}}{QH_2}$$

Q = I, VI, XI

Scheme 2. A possible route for the reductive activation of Q.

have been calculated utilizing the AM1 RHF (restricted Hartree–Fock) formalism for closed systems, and the UHF (unrestricted HF) and RHF half-electron (HE) formalisms for open-shell systems [15]. All input structures were minimized using PCMODEL [16] prior to AM1 calculations as implemented in AMPAC (v. 4.5, Semichem) [17]. Some calculations were also performed using MOPAC5 [18]. The molecular geometries and energies obtained from AMPAC involved BFGS (Broyden–Fletcher–Goldfab–Shanno) optimization with respect to all structural variables unless single-point calculations on specific geometries were of interest. Conformational energies were calculated by optimizing all parameters except the torsion angle of interest. The PRECISE option was used for all optimization. Energy-partitioning analysis was performed by specifying the option ENPART [17,18]. All RHF and UHF ab initio calculations were performed using SPARTAN (v. 3.1) [19] and GAUSSIAN92 [20] was used for ROHF ab initio calculations. Some AM1 calculations were also done using SPARTAN (v. 3.1) [19].

Calculation of reaction enthalpies

Reaction enthalpy calculations for electron attachment (REA) were accomplished by determining ΔH of the reaction $Y + e^- \rightarrow Y^-$, i.e., $REA_{calc} = Hf(Y^-) - Hf(Y) = \Delta H$, where Y is Q or $QH^\cdot$ and Hf is the calculated heat of formation. Reaction enthalpies for proton attachment (REP) were also calculated by determining ΔH of the reaction $Y + H^+ \rightarrow YH$, i.e., $REP_{calc} = \Delta H = Hf(YH) - Hf(Y)$, where Y is Q^- or QH^-.

TABLE 1
SELECTED BOND LENGTHS (Å) FOR VARIOUS REDOX STATES OF **I**, **VI** AND **XI**

Bond	Q	Q^-	$QH^\cdot$	QH^-	QH_2
I					
O1-C2	1.236	1.268	1.252	1.267	1.3785
C2-C3	1.479	1.447	1.461	1.445	1.407
C3-C4	1.338	1.362	1.373	1.375	1.387
C4-C5	1.479	1.447	1.423	1.404	1.407
C5-O6	1.236	1.268	1.366	1.391	1.3784
VI[a]					
O1-C2	1.237	1.268	1.251 (1.370)	1.267 (1.390)	1.379
C2-C3	1.475	1.446	1.460 (1.416)	1.444 (1.402)	1.403
C3-C4	1.339	1.363	1.37 (1.381)	1.373 (1.374)	1.387
C4-C5	1.481	1.446	1.434 (1.449)	1.415 (1.454)	1.415
C5-N6	1.290	1.339	1.379 (1.335)	1.428 (1.319)	1.404
XI					
N1-C2	1.291	1.334	1.333	1.324	1.405
C2-C3	1.478	1.447	1.448	1.447	1.412
C3-C4	1.339	1.362	1.377	1.378	1.387
C4-C5	1.479	1.446	1.428	1.409	1.412
C5-N6	1.291	1.334	1.372	1.403	1.405

[a] Values in parentheses are for isomers of $QH^\cdot$ and QH^-.

TABLE 2
CHANGES (Å)[a] IN SELECTED BOND LENGTHS AS A RESULT OF ELECTRON AND PROTON ATTACHMENTS

Bond	Q^-	$QH^\cdot$	QH^-	QH_2
I				
O1-C2	0.032	0.016	0.031	0.143
O2-C3	–0.032	–0.018	–0.034	–0.072
C3-C4	0.024	0.035	0.037	0.049
C4-C5	–0.032	–0.056	–0.075	–0.072
C5-06	0.032	0.13	0.155	0.142
VI[b]				
O1-C2	0.031	0.014 (0.133)	0.03 (0.153)	0.142
C2-C3	–0.029	–0.015 (–0.059)	–0.031 (–0.073)	–0.072
C3-C4	0.024	0.031 (0.042)	0.034 (0.035)	0.048
C4-C5	–0.035	–0.047 (–0.032)	–0.066 (–0.027)	–0.066
C5-N6	0.049	0.089 (0.045)	0.138 (0.029)	0.114
XI				
N1-C2	0.043	0.042	0.033	0.114
C2-C3	–0.031	–0.03	–0.031	–0.066
C3-C4	0.023	0.038	0.039	0.048
C4-C5	–0.033	–0.051	–0.07	–0.067
C5-N6	0.043	0.081	0.112	0.114

[a] Changes in bond lengths are relative to bonds in Q forms of **I**, **VI** and **XI**.
[b] Values in parentheses are for isomers of $QH^\cdot$ and QH^-.

Other derived quantities

Within the validity of Koopmans' theorem [21], the frontier orbital energies have been used to calculate absolute electronegativity (X) utilizing the formula for this quantity [22]: $X = (I + A)/2$, where I and A are the ionization potential and electron affinity of any chemical system, respectively, and are given by the negative of the energies of the HOMO and LUMO orbitals, respectively [23]. For a radical, $I = -e_{SOMO}$ (the negative of the SOMO orbital energy). HOMO, SOMO and LUMO are the highest occupied, singly occupied, and lowest unoccupied MOs, respectively. The electronic chemical potential is equal to the negative of X [24]. Other details for the calculation of adiabatic ionization potential (IP_{ad}), adiabatic electron affinity (EA_{ad}), adiabatic electronegativity (X_{ad}) and hardness (N_{ad}) are provided elsewhere [25].

Results and Discussion

*Geometrical reorganization: Comparison of 1,4-benzoquinone (**I**) and its analogs p-benzoquinone imine (**VI**) and p-benzoquinone diimine (**XI**)*

The reductive activation of the quinone moieties of the drugs should induce considerable reorganization in their electronic structures, which should in turn be manifested as changes in geometry (topology), ionization potential, electron affinity, electronegativety (or electronic chemical potential), etc. The reorganization in the electronic structures of **I**, **VI** and **XI** as they undergo the reactions in

TABLE 3
COMPARISON OF SOME BOND ANGLES[a] AND DIHEDRAL ANGLES[a] FOR DIFFERENT REDOX STATES OF I AND VI

	Q	$Q^{\cdot-}$	$QH^{\cdot}$	QH^{-}	QH_2
I					
Bond angles (°)					
O1-C2-C3	122	122.1	121.7	122.1	116.2
O12-C5-C4	122	122.1	116.2	120.0	116.2
C5-O6-H9			108.3	105.2	107.8
C5-C6-H8	115.7	116.8	119.3	118.8	120.4
Dihedral angles (°)					
H9-O6-C5-C4			180.0	91.7	179.8
VI					
Bond angles (°)					
O1-C2-C3	122.4	122.3	121.9	122.2	116.6
N6-C5-C4	119.6	120.1	120.9	122.6	120.6
C5-N6-H9	115.6	111.3	116.8	108.7	113.5
C5-N6-H10			116.8	108.7	113.5
C5-C7-H11	116.6	117.8	119.0	119	120.2
Dihedral angles (°)					
H9-N6-C5-C4	0.1	180	163.2	56.9	−156.6
H10-N6-C5-C4			20.2	58.7	−26.6

[a] Atom labeling as in Fig. 2.

Scheme 2 can be assessed by analyzing bond lengths, and bond and torsional angles, and selected relevant parameters are presented in Tables 1–3 (data for **XI** are not included here). Considering the bond lengths and changes thereof shown, similar trends are observed in going from $Q \rightarrow Q^{\cdot-} \rightarrow QH^{\cdot} \rightarrow QH^{-} \rightarrow QH_2$ (Schemes 2 and 3). The O1-C2 and C5-O6, and the N1-C2 and C5-N6 bond lengths are the same in **II** ($Q^{\cdot-}$) and **XII**, respectively, indicating the extensive electron delocalization (see Fig. 2 for numbering scheme). In radical anions **II** and **VII**, the O1-C2, C3-C4 and C5-O6 (**II**) and C5-N6 (**VII**) bond lengths increase with a concomitant decrease in the C2-C3 and C4-C5 bond lengths. A very similar trend is observed for $Q^{\cdot-}$ of **XI** (i.e., **XII**). This is an indication of considerable increase in the π-electron delocalization over the O1(or N1)-C2-C3-C4-C5-O6(or N6) fragment. Protonation of **II**, **VII** and **XII** to **III**, **VII** and **XIII**, respectively, increases C2-C3, C3-C4 and C5-O6 (or C5-N6) while a decrease is seen for O1-C2 and C4-C5 bond lengths; N1-C2 in **XII** and **XIII** is, however, about the same. The O1-C2 and N1-C2 bonds are the shortest bonds in the radicals, indicating that they are the most localized bonds. As can be seen in Table 3, salient changes are also observed in bond angles, although a clear trend is not manifested. On the other hand, all the torsional (dihedral) angles (most are not shown in Table 3) for **I–III** and **VI–VII** are either 0° or 180° while the dihedral angles containing the H's on the N atom in **VIII–X** (and in **XIII–XV** as well) deviate from 0° or 180° considerably; the same is true for the dihedral angle in IV (QH^{-}) (=91.7°). This is a clear indication that structures **I–III**, **VI** and **VII** are planar while the others are not. This observation further suggests that in those cases where there is considerable deviation from planarity, the hybridization must have changed considerably.

Energy-partitioning analysis

A detailed dissection of the total energies into one- and two-center terms can be used to explain why formations of **II** from **I**, and of **VIII** from **VII**. are more favorable over formations of **VII** from **VI** and of **III** from **II**, respectively. Such data along with data on contributions of one- and two-center energies of electron and proton attachments including two-center net destabilization and/or stabilization energies arising from electron and proton attachments are available as supplementary material. The net stabilization and/or destabilization energies are given by the sum of the one- and two-center terms. The analysis showed that the reason why the formation of **II** from **I** is favored over that of **VII** from **VI** is a result of the destabilizing effect of the two center neighboring pair interactions. A similar energy-partitioning analysis for the protonation process showed that the reason why the formation of **VIII** from **VII** is more favorable over that of **III** from **II** is a result of the stabilizing energy contribution due to the two-center neighboring pair interactions.

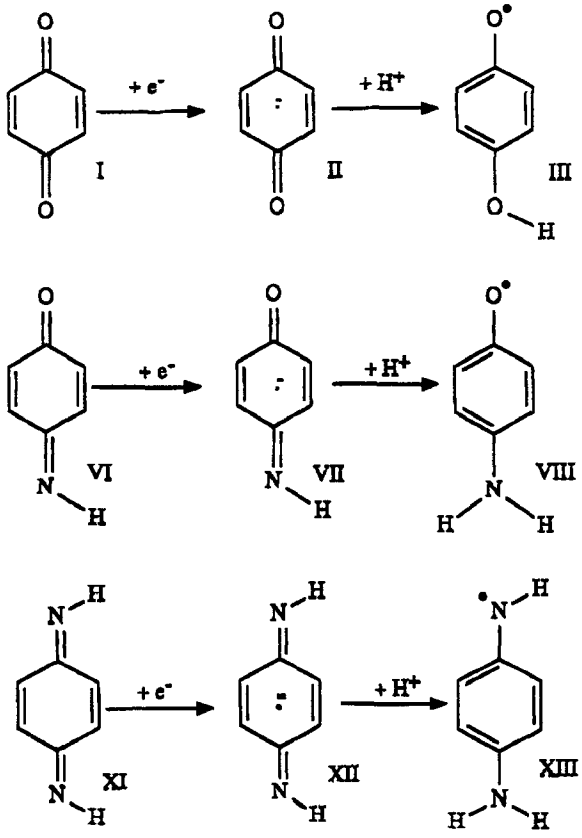

Scheme 3. Reductive activation of Q to $QH^{\cdot}$.

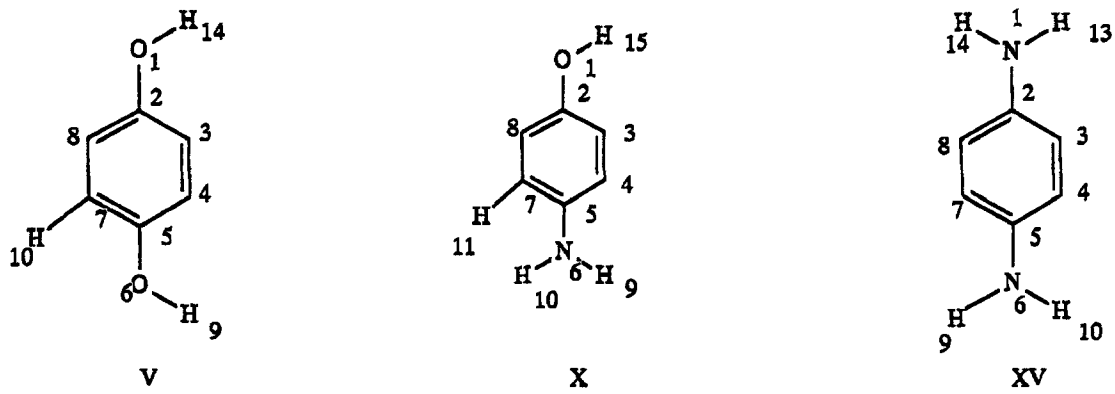

V X XV

Fig. 2. Atomic labeling. The redox states **1**–**5** in Scheme 2 are designated, respectively, **I**–**V** for 1,4-benzoquinone, **VI**–**X** for 1,4-benzoquinone imine, and **XI**–**XV** for 1,4-benzoquinone diimine.

The partitioning of the total energy seems to indicate that the favorability or unfavorability of electron and proton attachments in **I**, **VI** and **XI** is governed by the two-center neighboring pair interactions (i.e., considering interactions between atoms within 1.9 Å of each other). The data given in Tables 1 and 2 partially reflected the reorganization of the electronic structures of benzoquinone and its analogs as they undergo reductive activation. Further insight into these structural changes can be obtained from a quantification of interatomic interactions [26] via the energy-partitioning analysis technique [27]. Figure 3 shows some selected pair interactions from which an assessment of stabilizing (negative values) and destabilizing (positive values) effects can be determined. For bonding pair interactions, the magnitude of the energy, which is due to the contribution of the one-electron core resonance integrals to the energy of a bond, reflects the strength of the bond between the atoms of the pair [26,27]. It is evident from the data in Fig. 3 how the pair interactions change for the first two steps of Scheme 2. What is of interest is, of course, how these changes manifest themselves in the reactivity of the species resulting from the reduction. In modifying I to VI, a C5=O6 bond is replaced by C5=N6H. It has been pointed out earlier that the reason why the formation of **II** from **I** is more favorable than the formation of **VII** from **VI** is due to the greater destabilization effect of the two-center term in **VII**, and further analysis of the data showed that the greater portion of this destabilization effect apparently comes from the C5-N6 pair interactions.

In going from **II** to **III** and from **VII** to **VIII**, respectively, the C5-O6 group transforms to C5-O6H and the C5-N6H group to C5-N6H_2. Considering the two center bonds in these transformations, the net stabilizations from the two transformations can be computed. The results showed that the reason why proton attachment is more

TABLE 4
AM1 RHF/HE AND RHF/UHF[a] CALCULATED REACTION ENTHALPIES (kcal/mol) OF ELECTRON AND PROTON ATTACHMENTS AND COMBINATIONS THEREOF PERTAINING TO SCHEME 1

Step	I	VI	XI	Order[b]
Electron attachment				
1→2	−48.7 (−51.8)	−40.7 (−46.5)	−33.3 (−40.1)	I > VI > XI
3→4	−54.4 (−45.1)	−49.1 (−40.9)	−40.3 (−27.4)	I > VI > XI
Proton attachment				
2→3	41.6 (35.4)	24.7 (22.3)	18.5 (12.9)	XI > VI > I
4→5	20.9	18.6	1.2	XI > VI > I
Semiquinone formation				
1→3	−7.1 (−16.4)	−16 (−24.2)	−14.4 (−27.1)	VI > XI > I
Semiquinone anion formation				
1→4	−61.5	−65.1	−54.7	VI > I > XI
Hydroquinone formation				
1→5	−40.6	−46.5	−53.5	XI > VI > I
3→5	−33.5 (−24.2)	−30.5 (22.3)	−39.1 (−26.4)	XI > I > VI

[a] Values are those given in parentheses.
[b] Relative orders are the same for RHF/HE and RHF/UHF results except for semiquinone formation (1→3) for which the order is XI > VI > I.

favorable in **VII**, compared to that in **II**, is due to, by and large, the net stabilization energy involving the C-N and N-H bonds as a result of the transformation from **VII** → **VIII**. This net stabilization favors the reductive activation of **VI** to **VIII** as opposed to **I** to **III**. The reoxidation of QH$^{\cdot}$ to Q involves deprotonation and electron detachment processes. Deprotonation is less favorable in **VIII** and electron detachment is less unfavorable in **VII** (than in **III** and **II**, respectively). The energetics are, however, such that deprotonation outweighs the energetics of electron detachment and the overall reoxidation of **VIII** to **VI** is more unfavorable when compared to the reoxidation of **III** to **I**. The foregoing analysis suggests that redox cycling (reduction and autoxidation) in **VI** should be less favorable than that of **I** primarily due to differences in the energetics of electron attachment (to **I** and **VI**) and deprotonation (of **III** and **VIII**, i.e., the QH$^{\cdot}$ forms of **I** and **VI**, respectively) processes. Since redox cycling is presumed to play an important role in the biochemical activity of the drugs, the above findings may have a bearing on the reduced toxicity of 5IDN (vide infra).

Relative importance of electron and proton attachments

The AM1-calculated reaction enthalpies for the various electron and proton attachment steps according to Scheme 2, and for their combinations, are summarized in Table 4. Table 4 also provides the ease of electron or proton attachment for the various steps or combinations thereof in Scheme 2 in decreasing order. Several conclusions can be made from the data:

(1) Replacement of O by NH: (a) makes electron attachment less favorable, (b) makes proton attachment more favorable, and (c) the order for ease of electron attachment is the reverse of that of proton attachment.

(2) The trends for semiquinone and hydroquinone formations follow that of proton attachment.

(3) The trend for electron attachment to the semiquinone (QH$^{\cdot}$) (**3**→**4**) giving the semiquinone anion (QH^{-}) is different from the overall trend for QH^{-} formation (**1**→**4**).

(4) The trend for the overall hydroquinone (QH_2) formation (**1**→**5**) is different from that for the formation of QH_2 from QH$^{\cdot}$ (**3**→**5**).

(5) Since the trends for QH$^{\cdot}$ and QH_2 formation (**1**→**3**

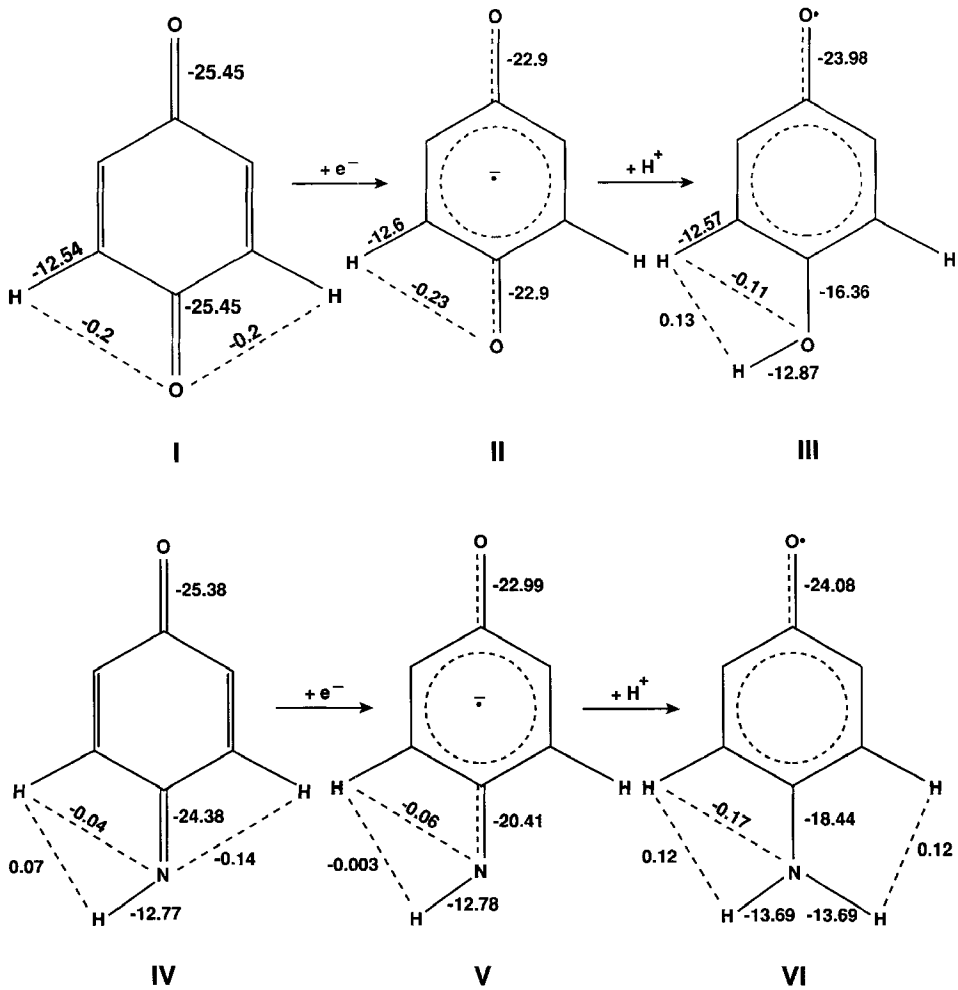

Fig. 3. Selected pair interactions (eV) showing stabilizing (negative values) and destabilizing (positive values) effects.

and **1**→**5**, respectively) follow the trend for proton attachment, proton attachment seems to govern the enthalpy of $QH^{\cdot}$ and QH_2 formation.

(6) The overall QH^- formation (**1**→**4**) and QH_2 formation from $QH^{\cdot}$ (**3**→**5**) are different from the patterns for the electron and proton attachment steps.

Possible reductive routes for the conversion of **VI** to the hydroquinone form (X) are shown in Scheme 4. The route in Scheme 2 is denoted by route A1 in Scheme 4 and it is evident from the overall reaction enthalpies that routes A1 and B1 are equally favorable (Scheme 4), although individual corresponding steps in the two routes are not. Route B1 is therefore a viable route in the reduction of **VI** to **X**. On the other hand, routes A2, A3 and B2 probably do not contribute to the overall reductive process as can be judged from the calculated reaction enthalpies for these routes. Conversion of the semiquinones ($QH^{\cdot}$) of **I** and **XI** can also take place via routes shown in Scheme 5, but these routes are not as favorable as the routes in Scheme 2. In any case, since the cationic radicals **7**, **8**, **9** and **10** (Schemes 4 and 5) are electron-deficient, they are not expected to transfer electrons to other species and are not considered further in this work, except to mention that if they do form, they can act as oxidizing agents.

Conformational energies of, and rotational barriers in, $QH^{\cdot}$, QH^- and QH_2

The effects of electron and proton attachments may lead to deviations from planarity and/or optimal ring

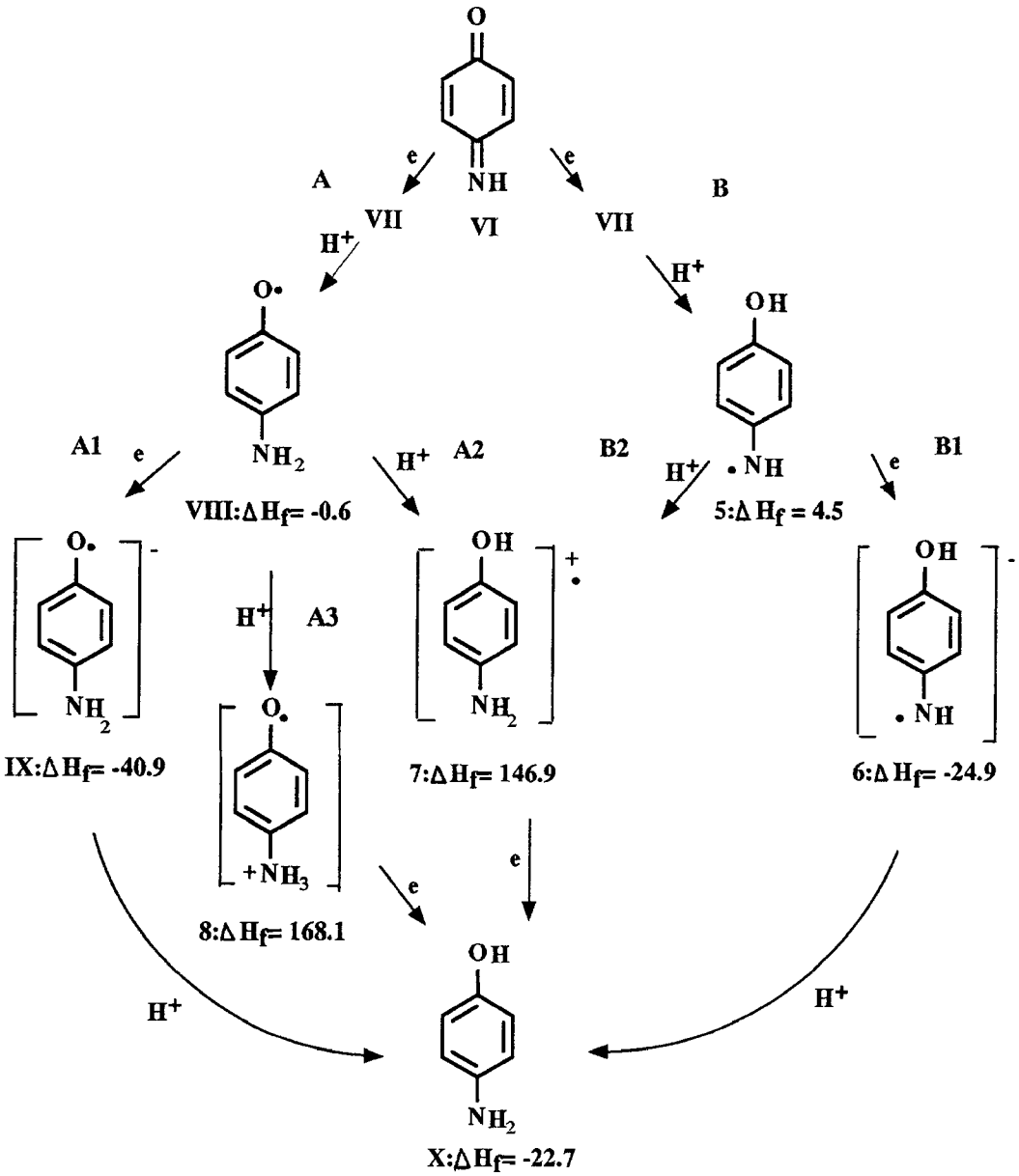

Scheme 4. Possible routes for the conversion of **VI** to **X**. ΔH_f's for **VI** and **VII** are given in Table 1.

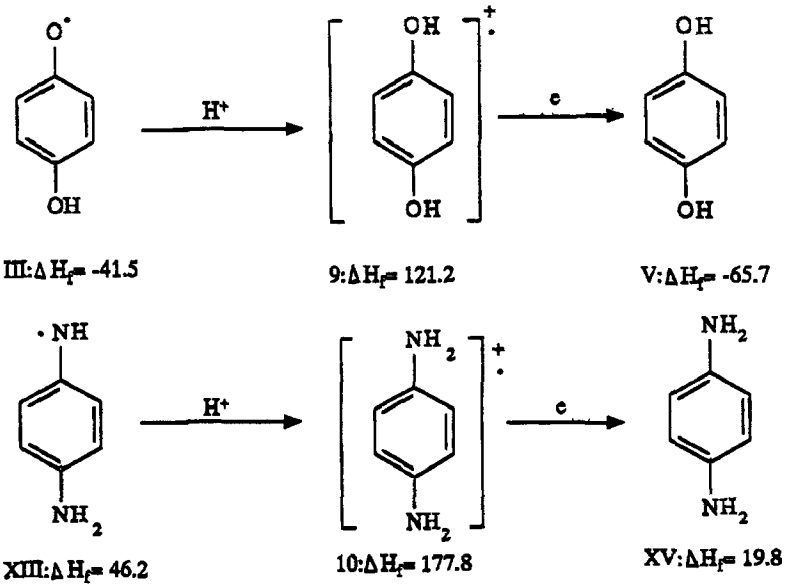

Scheme 5. Alternative routes for the conversion of the semiquinones of **I** and **XI** to **V** and **XV**, respectively.

conjugation and these effects can be assessed by conformational energy searches. Conformational energy searches were carried out for $QH^{\bullet}$, QH^{-} and QH_2 of **I**, **VI** and **XI** as well as for **5** and **6** (Scheme 4), the isomers of **VIII** and **IX**, respectively. The conformational energy scans were carried out with respect to rotation about bond C5-O6 in **I** (torsional angle: H9-O6-C5-C4); bond C5-N6 in **VI** (torsional angle: H9-N6-C5-C4), bonds C2-O1 (torsional angle: H15-O1-C2-C3) and C5-N6 (torsional angle: H9-N6-C5-C4) in **5** and **6**, and bonds C2-N1 (torsional angle: H13-N1-C2-C3) and C5-N6 (torsional angle: H9-N6-C5-C4) in **XI** (the atom numbering used is that of Fig. 2 and H14, H15, H10 and H14 are not present in the redox states $QH^{\bullet}$ and QH^{-} of **I**, **VI**, **5** (or **6**) and **XI**, respectively). All coordinates except the torsional angle under consideration were optimized during the conformational searches. Conformational energies relative to the energy of the conformation with the lowest energy are presented in Table 5 for selected torsional angles. The p's against the 0° and 180° torsional angles indicate planar conformations. While some of these are minima (assigned 0.0 kcal/mol), others are not. For QH^{-} of **I**, the 0° and 180° torsion angle conformations are planar transition states and the minimum-energy conformation of QH^{-} of **I** has a torsional angle (H9-O6-C5-C4) of 90°. The 0° and 180° torsion angle conformations of $QH^{\bullet}$ and QH^{-} of **VI,i** (**5** and **6**, Scheme 4) are planar but not minima. In **XI**, the 0° and 180° torsion angle conformations are not planar although some of them are minima. Except for QH_2 of **I**, all other QH_2's are nonplanar.

Comparison of the conformational energy profiles (not shown) of **I** and **VI,i** (where the torsional angle for **VI,i** under consideration was H15-O1-C2-C3) showed that rotations about bond C2-O1 in **I** and **VI,i** gave very similar energy profiles. Profiles for rotations with respect to C-NH_2 (for **VI** and **XI**) and C-NH (for **VI,i** and **XI**) also gave similar profiles. Table 6 summarizes the rotational barriers extracted from the energy profiles. It is evident that rotations about C-OH in **I** and **VI,i**, and about C-NH_2 in **VI** and **XI**, have comparable rotational barriers. The rotational barriers about bond C-NH in **VI,i** and **XI** are also comparable but substantially higher than those of the C-OH and C-NH_2 cases for redox states $QH^{\bullet}$ and QH^{-}. A probable explanation for this relatively high energy barrier is that rotation about bond C-NH in $QH^{\bullet}$ and QH^{-} of **VI** and **XI** leads to a substantial loss of ring conjugation.

Both the Q and $Q^{\bullet-}$ forms of **I**, **VI** (or **VI,i**) and **XI** are planar. Attachment of the first electron (to Q forms) does not apparently change the planarity of the parent molecule but leads to greater ring conjugation in the $Q^{\bullet-}$ forms as manifested by the lengthening of the double bonds in Q by about 0.02–0.032 Å, and by the shortening of the C–C single bonds in Q by about 0.03–0.035 Å (Table 2). In $QH^{\bullet}$, QH^{-} and QH_2 forms, however, not all minimum energy conformations have 0° and 180° torsional angles and most of the other minimum energy conformations occur with a deviation of about ±20° from 0° and/or 180° torsional angles.

Comparison of reducibility and oxidizability of I and VI and their redox states

The data in Table 4 on reaction enthalpies for electron and proton attachments and combinations thereof show that reductive activation to both the semiquinone ($QH^{\bullet}$) and the hydroquinone (QH_2) forms (which involves both electron and proton attachments) is more favorable in **VI** than in **I**. This is primarily due to the greater proton affinity of **VI** (and its redox states) since the reaction enthalpies for the electron attachment steps are more

TABLE 5
CONFORMATIONAL ENERGIES OF QH', QH⁻ AND QH_2 FORMS OF **I**, **VI**, **VI,i**[a] AND **XI** RELATIVE TO THE ENERGY OF THE MINIMUM ENERGY CONFORMATION FOR SELECTED TORSIONAL ANGLES[b]

Rotational bond	Torsional angles (°)					
	−20	0	60	90	160	180
I C_5-O_6H						
QH'	0.3	**0.0** p	2.5	3.6	0.4	0 p
QH⁻	1.1	1.26 p	0.3	**0.0**	1.1	1.3 p
QH_2	0.2	**0.0** p	1.3	1.9	0.3	**0.05** p
VI C_5-N_6H2						
QH'	**0.0**	0.38	2.1	5.1	**0.01**	0.4
QH⁻	0.4	0.3	**0.0**	0.1	0.4	0.3
QH_2	**0.04**	0.7	3.1	2.5	**0.0**	0.6
VI,i C_2-O_1H						
QH'	0.42	0.13 p	2.2	3.1	0.35	**0.0** p
QH⁻	1.5	1.67 p	0.47	**0.0**	1.41	1.62 p
QH_2	0.16	**0.0**	1.32	1.8	0.26	**0.0**
VI,i C_5-N_6H2						
QH'	1.53	0.13 p	10.32	14.2	1.65	**0.0** p
QH⁻	1.61	**0.0** p	13.01	22.1	1.87	**0.05** p
QH_2	**0.04**	0.7	3.1	2.5	**0.0**	0.6
XI C_2-N_1H						
QH'	1.4	**0.0**	10.45	14.9	1.7	**0.0**
QH⁻	1.66	**0.0**	13.62	23	2.5	0.55
QH_2	**0.0**	0.67	3.0	2.42	0.14	0.67
XI C_5-N_6H2						
QH'	**0.01**	0.71	1.54	4.0	**0.0**	0.55
QH⁻	0.54	0.4	**0.0**	0.15	0.54	0.4
QH_2	**0.0**	0.67	3.0	2.42	0.14	0.67

[a] QH' and QH⁻ of **VI,i** are, respectively, structures **5** and **6** (Scheme 4); QH_2 of **VI,i** is the same as QH_2 of **VI**.
[b] p's indicate planar conformations.

favorable in **I**. Based on these results, one might be inclined to suggest that the net effect of the alteration of the quinone site in DN to that in 5IDN might lead to an apparent enhanced reducibility in 5IDN. The reducibility and oxidizability of **I** and **VI** (as well as **XI**) and their redox states can be further assessed by examining the data on adiabatic electron affinity (EA_{ad}), adiabatic ionization potential (IP_{ad}), and adiabatic electronegativity and hardness (X_D and N_D, respectively). These data are presented in Table 9 in a manner that makes the comparison easy.

Electron affinity (EA_{ad}) and ionization potential (IP_{ad})

Using the data in Table 7, a qualitative to semiquantitative comparison of **I**, **VI** and **XI** and their respective redox states can be made. The EA_{ad} data clearly indicate a decreasing order in EA_{ad} of QH' > Q > QH_2 > Q⁻ > QH⁻. Since the EA_{ad}'s of QH' and Q are relatively comparable, the difference being less than 10 kcal/mol, QH' and Q have apparently comparable electron affinity. That the reduction product of Q, i.e., QH', has an EA_{ad} comparable to, actually even greater than, the electron affinity of Q is rather interesting. When a given redox state, e.g., QH', of **I**, **VI** and **XI** is considered, the differences between the EA_{ad}'s are not substantial. Thus, while a decreasing trend in EA_{ad} of **I** > **VI** > **XI** may be suggested by the data, the differences in the EA_{ad}'s of **I**, **VI** and **XI** (and their corresponding redox states) may not be sufficient to conclude that the electron affinity of VI is substantially diminished relative to that of I. Similarly, examination of the IP_{ad} data in Table 7 may point to a decreasing trend Q > QH_2 > QH' > QH⁻ > QH⁻ in IP_{ad}. However, it is apparent from the data that the IP_{ad}'s of QH_2 and QH', as well as those of QH⁻ and Q⁻, are relatively comparable. Again, for a given redox state, while a decreasing trend **I** > **VI** > **XI** in IP_{ad} is suggested, the differences in IP_{ad} of a given redox state are not very large, particularly for QH⁻ and Q⁻ of **I**, **VI** and **XI**. For QH_2 and QH' of **I** and **VI**, the differences in IP_{ad} are about 15 and 20 kcal/mol and, given the approximations used in the methods, they may not be considered very large. However, the data overall clearly demonstrate that **VI** is, if not more oxidizable, as oxidizable as **I**.

Adiabatic electronegativity (X_{ad}) and hardness (N_{ad})

The X_{ad} data presented in Table 7 suggest a decreasing order Q > QH' > QH_2 > Q⁻ > QH⁻ for each system (i.e., **I**, **VI** and **XI**), and for a given redox state (e.g., QH') the de-

TABLE 6
COMPARISON OF ENERGY BARRIERS[a] TO INTERNAL ROTATION (kcal/mol)

Rotational bond	QH'	QH⁻	QH_2
I			
C5-O6H	3.6	1.3	1.9
VI,i			
C2-O1H	3.1	1.7	1.8
VI			
C5-N6H2	0.4	0.4 6.7	3.1
VI,i			
C5-N6H	14.2	22.1	3.1
XI			
C2-N1H	14.9	23.0	3.0 (1.6)[b] (20.0)[b]
C5-N6H2	0.7	0.5 5.2	3.0

[a] Values were obtained from plots of conformational energy profiles (not shown).
[b] Determined with the NH_2 group kept frozen and planar with the ring.

TABLE 7
AM1 CALCULATED IP_{ad}, EA_{ad}, X_{ad} AND N_{ad} FOR **I**, **VI**, **XI** AND THEIR RESPECTIVE REDOX STATES[a]

Energy	Q	QH_2	$QH^{\cdot}$	QH^-	$Q^{\cdot-}$
IP_{ad}					
I	244.4	189.7	184.8	54.4	48.9
VI	233.1	174.1	162.1	49.1	40.7
(VI,i)[b]			(173.0)	(44.2)	
XI	217.0	161.6	157.7	40.3	32.9
EA_{ad}					
I	48.7	3.9	53.4	−113.7	−74.9
VI	40.7	0.3	49.1	−115.5	−80.5
(VI,i)[b]			(44.2)	(115.2)	
XI	32.9	−3.9	40.3	−117.2	−85.4
X_{ad}					
I	146.6	96.8	119.1	−29.7	−13.0
VI	136.9	88.2	105.6	−33.0	−19.9
(VI,i)[b]			(108.6)	(−35.5)	
XI	125.0	78.9	97.0	−38.5	−26.3
N_{ad}					
I	97.9	92.6	65.7	84.1	61.9
VI	96.2	86.9	56.5	82.1	60.6
(VI,i)[b]			(56.7)	(79.7)	
XI	92.1	82.7	64.4	78.8	59.2

[a] All values are in kcal/mol.
[b] Values are for structures **5** and **6** (Scheme 4).

creasing order in X_{ad} is **I** > **VI** > **XI**. As shown elsewhere [25], the calculated X_{ad} and X_v are in very close agreement and these may suggest that the trends observed are reasonably reliable. Since lower electronegativity values reflect a greater tendency to lose electrons, the reverse of the above orders gives a decreasing order in the tendency to lose electrons. It thus appears that the redox states of **VI** should be more oxidizable than the corresponding redox states of **I**. In the case of the N_{ad} data, a decreasing order $Q > QH_2 > QH^- > QH^{\cdot} > Q^{\cdot-}$ may be suggested. However, some of the redox states do not show significant differences in their N_{ad} values. In particular, the N_{ad} values of QH_2 and QH^-, as well as those of $QH^{\cdot}$ and $Q^{\cdot-}$, are relatively close. Thus, the reactivity of QH_2 and $QH^{\cdot}$ should be similar to that of QH^- and $Q^{\cdot-}$, respectively. It is, however, of interest to compare QH_2 (and/or QH^-) with $QH^{\cdot}$ (and/or $Q^{\cdot-}$). At least in the case of **I** and **VI**, the difference in the N_{ad} values for QH_2 and $QH^{\cdot}$ is almost 30 kcal/mol. This should suggest that $QH^{\cdot}$ ought to be more reactive than QH_2. On the other hand, the N_{ad} values of a given redox state (e.g., $QH^{\cdot}$) of **I**, **VI** and **XI** do not seem to vary significantly. Thus, notwithstanding the fact that the HOMO–LUMO gap has been attributed to be a good indicator of reactivity, the data do not suggest that corresponding redox states of **I**, **VI** and **XI** have significant differences in reactivity as judged by the hardness data.

Discussion

Redox capacity

The capacity of 5IDN to form reactive radical species following the metabolic reduction known to activate both adriamycin and daunomycin (DN) depends on the reducibility of 5IDN and the oxidizability of the reduced form of 5IDN [11]. Assessing this capacity by using IP_{ad}, X_{ad} and N_{ad} data to compare the reducibility and oxidizability of **I** and **VI** and their corresponding redox states suggests that **VI** (hence 5IDN) should not have a diminished capacity to form reactive radical species, i.e., from molecular oxygen. The conformational energy analysis of the reduced forms of **I** and **VI** ($QH^{\cdot}$, QH^- and QH_2) points out that significant and salient changes arise as a result of electron and proton attachments. The rather small differences in the geometrical reorganizations of **I** and **VI** arising from the reductive activation are not, however, thought to lead to significant diminution in the redox capacity of **VI** (and hence 5IDN).

The energy-partitioning analysis and the data in Table 4 on reaction enthalpies for electron and proton attachments and combinations thereof and the electron affinity data show that reductive activation to both the semiquinone ($QH^{\cdot}$) and the hydroquinone (QH_2) forms is more favorable in **VI** than in **I**. This is primarily due to the greater proton affinity of **VI** since the reaction enthalpies for the electron attachment steps are more favorable in **I**. Based on these results, one might be inclined to suggest that the net effect of the alteration of the quinone site in DN to that in 5IDN should lead to an apparent enhanced reducibility in 5IDN. The first step of the reductive activation is electron attachment; this is, however, less fa-

TABLE 8
AM1- AND AB INITIO-CALCULATED DIPOLE MOMENTS (D) FOR REDOX STATES OF **I** AND **VI**

Redox state	AM1		HF/3-21G*		HF6-31G*//HF/3-21G*	
	I	**VI**	**I**	**VI**	**I**	**VI**
Q	0.019	2.319	0.001	2.861	0	2.75
$Q^{\cdot-}$	0.042	2.182	0.002	3.73	0	3.98
$QH^{\cdot}$	3.276	5.411	2.957	4.47	3.12	4.69
QH^-	4.734	5.613	6.051	6.76	6.35	6.924
QH_2	0.016	2.354	0	2.51	0	2.336

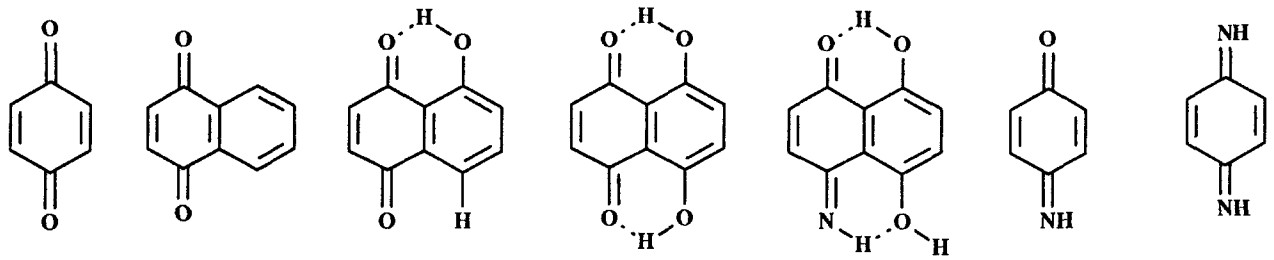

I XVI XVII XVIII XIX VI XI

Fig. 4. One- and two-ring model systems for anthracyclines. **I** = 1,4-benzoquinone; **XVI** = 1,4-naphthoquinone; **XVII** = 5-hydroxy-1,4-naphthoquinone (juglone); **XVIII** = 5,8-dihydroxy-1,4-naphthoquinone; **XIX** = 5,8-dihydroxy-1,4-naphthoquinone imine; **VI** = 1,4-benzoquinone imine; **XI** = 1,4-benzoquinone diimine. All except **XI** are part of the anthracycline pharmacophore; specifically, **XVII** is part of aclacinomycin A, **XVIII** is part of adriamycin and daunomycin, and **XIX** is part of 5-iminodaumycin.

vored in **VI**. Even though the differences in the proton affinity of **I** and **VI** are not very large, the estimated differences may suggest a significant difference in reducibility. On the other hand, the first step of the reoxidation is likely to be deprotonation and this is also less favored in **VI**. The overall effect of the reduced electron affinity and the enhanced proton affinity in **VI** may thus be to diminish the redox cycling of **VI** significantly.

Overall, the data show the relative trends in electron and proton attachment in the reductive activation of quinone and its isoelectronic analogs. If it is assumed that the radical species $Q^{\cdot-}$ and/or $QH^{\cdot}$ are responsible for toxicity, substitution with N should lead to a reduction in toxicity for two possible reasons: (i) less of the reduced species, $Q^{\cdot-}$, should form in the N-substituted case; and (ii) once $Q^{\cdot-}$ is formed it can be protonated more readily in the N-substituted case to form $QH^{\cdot}$, and if deprotonation of $QH^{\cdot}$ is essential for electron transfer to molecular oxygen as indicated in the proposal scheme for membrane lipid peroxidation and/or DNA damage (see the Introduction), the less favorable deprotonation in the N-substituted case should mean that less of $QH^{\cdot}$ would react to form reactive radical oxygen species such as $HO_2^{\cdot}$. The calculations of course did not incorporate medium effects due to hydration, pH and hydrophobic environments and the results may not allow one to reach definitive conclusions. For example, the calculated dipole moments of the various redox states might be considered to assess the influence of medium effects. Based on the data in Table 8, there are considerable differences in the dipole moments of the corresponding redox states of **I** and **VI**. Since the dipole moments of Q, $Q^{\cdot-}$ and QH_2 of **I** are essentially zero, whereas those of **VI** have dipole moments greater than 2 D, the interaction of these redox states of **I** and **VI** with charged and neutral species and with dipoles should be different. Similarly, the deprotonation of $QH^{\cdot}$ of **I** may be much more feasible under physiological pH conditions, whereas the deprotonation of $QH^{\cdot}$ of VI may require substantially higher pH values. Similarly, due to differences in the electronegativities of O and N, the stability of the $Q^{\cdot-}$ forms of **I** and **VI** might be quite different, particularly in hydrophobic medium. These calculations may, thus, be instructive in giving some insight into the rational design of imino- and amido-derivatives of quinone and anthraquinone containing drugs [28].

Trends in redox capacity due to ring expansion and substitution

The work presented in the previous paper [25] had indicated that semiempirically determined parameters can be used to establish trends in redox capacity. As an extension of this idea, it is of interest to examine the trends in the redox capacity of the model systems in Fig. 4. In Table 9 and Fig. 5, it is seen that expansion of the ring system as in **XVI** decreases IP_{ad}, EA_{ad} and X_{ad}. The increase in the HOMO and LUMO orbital energies is also consistent with this observation. Addition of the hydroxyl groups in **XVII** and **XVIII** decreases further the ionization potential (and increases the HOMO energy) but increases the electron affinity (consistent with the decreases in the

TABLE 9
SELECTED ENERGETIC PARAMETERS[a] FOR THE MODEL SYSTEMS IN FIG. 4

Energy	I	XVI	XVII	XVIII	XIX	VI	XI
HOMO	−10.876	−10.257	−9.621	−9.201	−9.113	−10.463	−9.766
LUMO	−1.735	−1.547	−1.675	−1.788	−1.353	−1.372	−1.031
IP_{ad}	244.4	223.1	208	197.7	177.4	233.1	217
EA_{ad}	48.7	45.3	48.9	52.1	49.8	40.7	32.9
X_{ad}	146.6	134.2	128.5	124.9	113.6	136.9	125

[a] HOMO and LUMO energies are in eV and all other parameters are in kcal/mol.

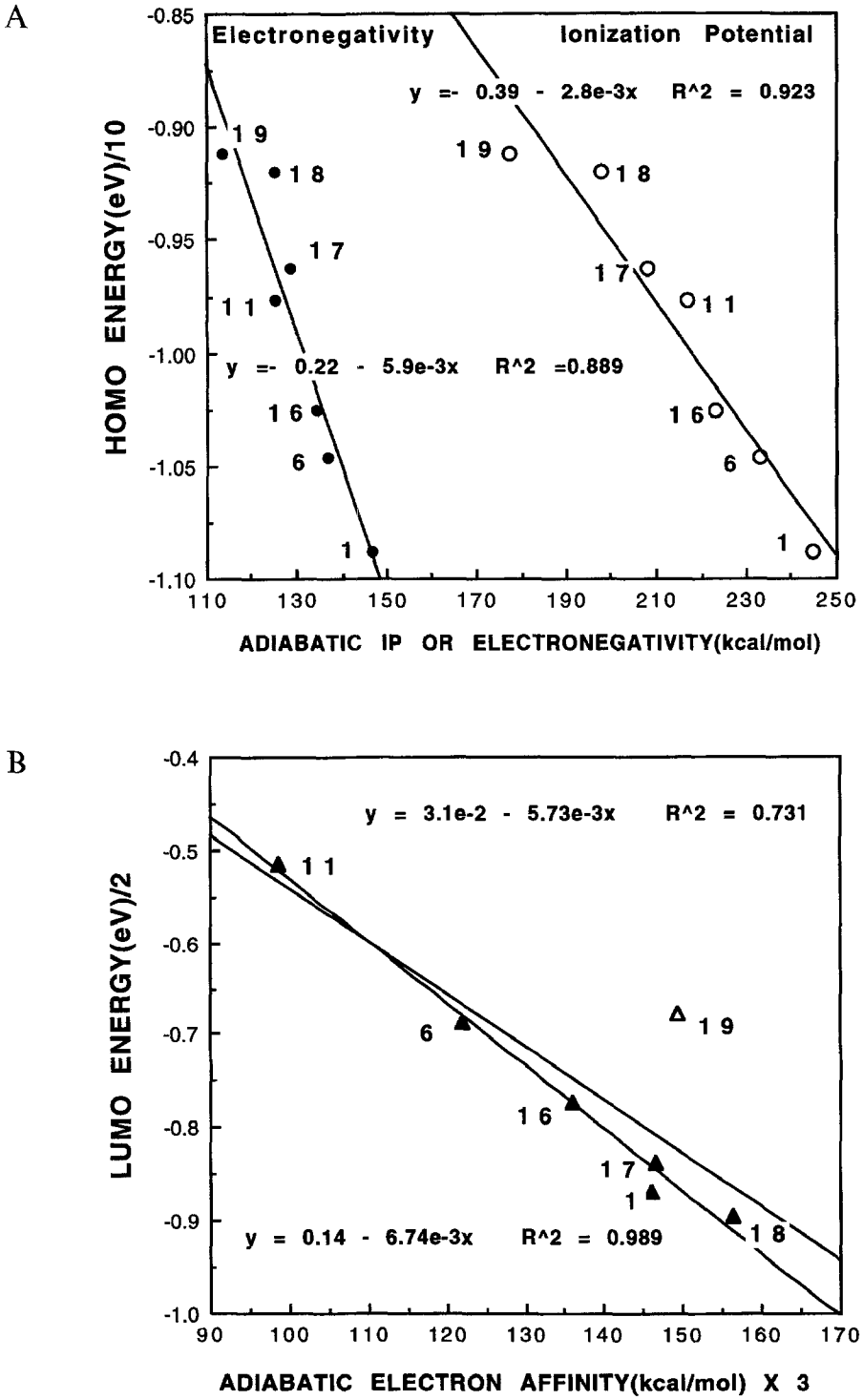

Fig. 5. (A) Correlation plots of HOMO orbital energy versus adiabatic IP or electronegativity. (B) Correlation plot of LUMO orbital energy versus adiabatic EA; the higher coefficient is obtained when 19 is excluded from the set. Data points are labeled in arabic numbers which correspond to the numbers in Table 9.

LUMO energy). The trend in going from **XI** to **VI** and to **XIX** is also similar. The data clearly indicate that the modification of **XI** to **VI** has the opposite effect of modifying **I** to **VI**. The increase or decrease in HOMO and LUMO energies can be interpreted in terms of trends of nucleophilicity and electron affinity. For example, the increase in the HOMO energies of **VI** and **XIX** relative to that of **I** and **XVIII**, respectively, implies increasing nucleophilicity [29] while the increase in the LUMO energies of **VI** and **XIX** relative to that of **I** and **XVIII** implies a decrease in electron affinity [25,30]. The value reported for **XIX** is for one of five structures with a heat of forma-

TABLE 10
AB INITIO-CALCULATED ENERGIES FOR ELECTRON AND PROTON ATTACHMENTS (kcal/mol)

	HF/3-21G*		HF/6-31G*//HF/3-21G*	
	I	**VI**	**I**	**VI**
Electron attachment				
1→2	−22.9 (−12.1)	−13.5 (−3.9)	−16.6	−10.2
3→4	12.2 (−2.2)	17.1 (3.7)	5.4	6.3
Proton attachment				
2→3	−363.9 (−360.4)	−376.6 (−380.2)	−354.9	−369.4
4→5	−384.1	−380	−370.4	−369.6
Semiquinone formation				
1→3	−386.8 (−372.5)	−390.1 (−384.1)	−371.5	−379.6
Semiquinone anion formation				
1→4	−374.6 (−374.7)	−373.0 (−380.4)	−366.1	−373.3
Hydroquinone formation				
1→5	−758.7	−753.0	−736.5	−742.9
3→5	−371.9 (−386.3)	−362.9 (−376.3)	−365	−363.3

tion of 53.1 kcal/mol (shown in Fig. 4). We have recently identified a more stable structure for **XIX** with an AM1 heat of formation of −62.7 kcal/mol. The AM1 HOMO and LUMO orbital energies for this structure are −8.47 and −1.489 eV (**XIX** is being investigated using different levels of theory and the results will be reported elsewhere). Compared to **XVIII**, all the different forms of **XIX** have lower IPs and EAs as assessed from their HOMO and LUMO orbital energies.

Further comparison of I and VI: Ab initio results

The overall suppression of redox cycling in **VI** predicted by the AM1 results is consistent with the experimental observation [11–13], but the results from ab initio calculations were deemed necessary to put the computational results on firmer ground.

Energies for electron and proton attachments

Hartree–Fock energies (HF/3-21G* and HF/6-31G*// HF/3-21G*) for electron and proton attachments calculated for this purpose are provided in Table 10. The ab initio energies are in general agreement with the AM1 results and the primary difference between the two cases (**I** and **VI**) is in the first electron attachment step (**1→2**) and in the proton attachment step **2→3**. The data in parentheses at the HF/3-21G* level are for ROHF calculations. The difference in the protonation energy of **I** and **VI** (more specifically **II** and **VII**) is of the order of 15–20 kcal/mol and is in good agreement with the AM1 results. The difference in the electron attachment energy (**1→2**), however, is about 6–8 kcal/mol, and this suggests that deprotonation may play a rather important role in the redox cycling process.

TABLE 11
AM1- AND AB INITIO-CALCULATED ELECTROSTATIC POTENTIAL MINIMA (V_{min}) AND MAXIMA (V_{max}) (kcal/mol)

Potential energy	AM1		HF/3-21G*		HF/6-31G//HF/3-21G*	
	I	**VI**	**I**	**VI**	**I**	**VI**
V_{min}						
Q	−50.8	−57.2	−42.6	−49.7	−36.4	−43.6
Q^-	−165	−174.3	−137.8	−153.9	−133.3	−149.1
$QH^\cdot$	−60.3	−66.9	−42.1	−46.7	−37.3	−41.9
QH^-	−184.4	−186.7	−162.9	−163.7	−155.9	−156.1
QH_2	−50.3	−55.9	−46	−59	−36.2	−40.85
V_{max}						
Q	23.8	37.1	39.3	60.2	37.3	54.7
Q^-	−67.6	−62.4	−62.8	−40	−62.2	−39.6
$QH^\cdot$	49.1	40.8	85.6	63	81.3	62.8
QH^-	−47.4	−47.7	−11.5	−34.7	−9.5	−33.95
QH_2	39.8	34.3	79.7	74.2	76	71.31

TABLE 12
TOTAL SPIN DENSITIES ON HEAVY ATOMS

Atom	Structure			
	II	**VII**	**III**	**VIII**
O1	0.399	0.235	0.816	0.797
C2	−0.024	0.235	−0.690	−0.654
C3	0.069	−0.298	0.811	0.767
C4	0.07	0.465	−0.723	−0.693
C5	−0.024	−0.461	0.723	0.669
O6 (N6)[a]	0.399	(0.783)	0.02	(0.072)
C7	0.068	0.483	−0.732	−0.693
C8	0.07	−0.367	0.792	0.768

[a] O6 in **II** and **III**; N6 in **VII** and **VIII**; atom labeling as in Fig. 2.

Electrostatic potential (V(r))

The reactivities of the redox states of **I** and **VI** can also be compared using electrostatic potentials (V(r)) [31], the calculated values (minimum (V_{min}) and maximum (V_{max})) for which are given in Table 11. All redox states of **VI** have stronger negative regions (V_{min}), which suggests that the redox states of **VI**, with the exception of QH^-, should be more susceptible towards electrophilic attack. The $Q^{\cdot-}$ forms of **I** and **VI** also have fairly strong negative V_{max} regions, while the V_{max} regions for the QH^- forms are relatively weaker negative regions. Q, $QH^{\cdot}$ and QH_2 have fairly strong to strong positive V_{max} regions. These positive V_{max} regions are in the vicinity of, and/or due to, H atoms (C-H, O-H and N-H groups), and although the H atoms themselves may not be specific sites for nucleophilic attack, they should enhance the electrophilicity of the regions in their immediate vicinity. For Q and $Q^{\cdot-}$, the V_{max} regions are the C-H (for **I**) and the N-H (for **VI**) regions, and the N-H regions are more susceptible to nucleophilic attack. For $QH^{\cdot}$ and QH^-, the V_{max} regions are due to O-H in **I** and N-H in **VI**, and $QH^{\cdot}$ and QH^- of **I** are more susceptible to nucleophilic attack. The V_{min} for the redox states of both **I** and **VI** are on the oxygen atoms, which is probably due to the lone pairs of the oxygen atoms. The relative electrophilicity of the carbonyl functionality in **I** and **VI** (i.e., Q) can be compared by considering the V_{min} values, and, in agreement with previous data, the V_{min} value for Q of **I** compared to that of **VI** indicates that the carbonyl functionality in **I** should be more susceptible to nucleophilic attack such as electron attachment (**1**→**2**). The V_{max} for $QH^{\cdot}$ and QH^- are substantially more positive for **I** than for **VI** (due to O-H and N-H, respectively), which does suggest that deprotonation of $QH^{\cdot}$ and QH^- of **I** should be more feasible. This quali-

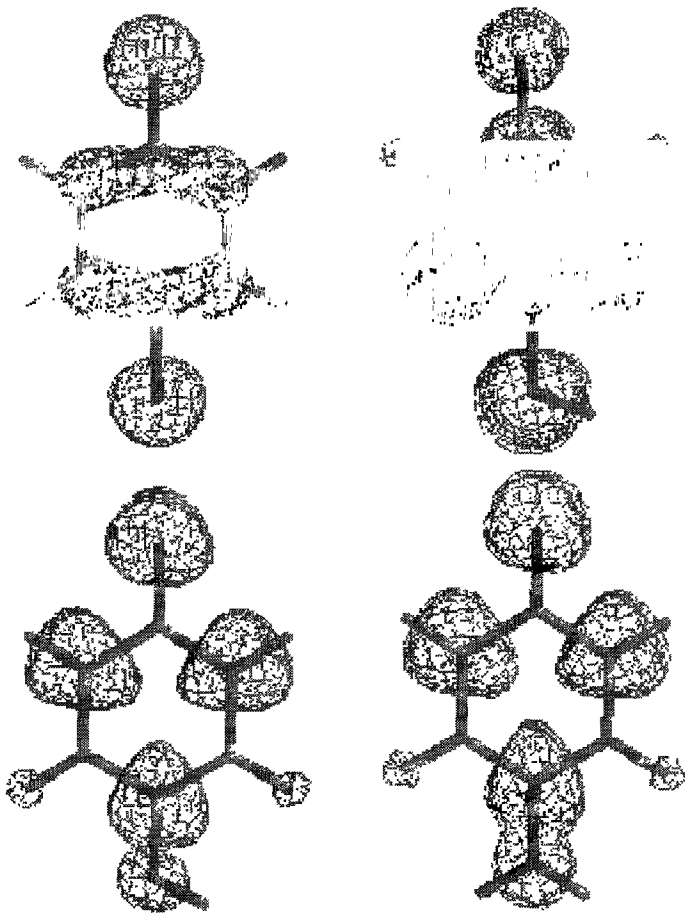

Fig. 6. Spin-density surfaces for **II**, **III**, **VII** and **VIII**.

TABLE 13
COEFFICIENTS OF THE $p_{x,y,z}$ BASIS FUNCTIONS GIVING RISE TO THE α-HOMOs OF II AND VII (6-31G* BASIS SET)[a]

Atom	II			VII
	$2p_x(3p_x)$	$2p_y(3p_y)$	$2p_z(3p_z)$	$2p_z(3p_z)$
O1	−0.12 (0.12)	−0.17 (−0.17)	0.11 (0.11)	0.31 (0.31)
C2	0.13 (0.11	0.19 (0.15)	−0.12 (−0.1)	−0.27 (−0.23)
C3	0.09 (0.1)	0.12 (0.14)	−0.08 (−0.09)	−0.2 (−0.23)
C4	−0.09 (−0.1)	−0.12 (−0.14)	0.08 (0.09)	0.16 (0.19)
C5	−0.13 (−0.11)	−0.18 (−0.15)	0.12 (0.1)	0.2 (0.18)
O6[b]	−0.12 (0.12)	0.17 (0.17)	−0.11 (−0.11)	−0.19 (−0.2)
C7	−0.09 (−0.1)	−0.12 (−0.14)	0.08 (0.09)	0.15 (0.16)
C8	0.09 (0.1)	0.12 (0.14)	−0.08 (−0.09)	−0.17 (−0.2)

[a] Atom labeling as in Fig. 2; contributions from orbitals on H's are negligible.
[b] N6 in **VII**.

tative assessment based on electrostatic potentials is again consistent with the suppression of redox cycling in **VI**.

Spin densities

Finally, since spin density is an indicator of the reactivity of radicals, it is of interest to compare the spin densities of $Q^{\cdot-}$ and $QH^{\cdot}$ of **I** and **VI** (Table 12). The spin densities of the heavy atoms of $Q^{\cdot-}$ of **I** (i.e., **II**) are shown to be less than 0.1 (and for the H atoms as well, not shown) except for the O atoms, whose spin densities are about 0.4. The spin densities of the heavy atoms in the case of $Q^{\cdot-}$ of **VI** (i.e., **VII**), however, are substantially different in magnitude (differences are observed in sign as well) and the highest spin density is on the N atom. The electrophilic site, as judged by the positive V_{max} of **VI**, is due to the N-H group, and the greater spin density at the N atom might be explained by the electrophilicity of the N-H region. The magnitudes of the spin densities for $QH^{\cdot}$ of **I** and **VI** are very similar, and a large preponderance of spin density on one atom is not evident in the $QH^{\cdot}$ forms. The spin-density distribution of the $Q^{\cdot-}$ and $QH^{\cdot}$ forms can be assessed better from the spin-density surfaces shown in Fig. 6. While the spin-density surfaces of the $QH^{\cdot}$ forms (**III** and **VIII**, respectively) of **I** and **VI** are very similar, there are clear differences in the spin densities of **II** and **VII** ($Q^{\cdot-}$ forms of **I** and **VI**). Since spin density is an indicator of reactivity for free radicals [32], the similarity of the spin densities of III and VIII ($QH^{\cdot}$ forms) suggests that **III** and **VIII** may have similar reactivity. On the other hand, the spin-density surfaces of **II** and **VII** indicate a marked difference in the distribution of unpaired electrons, and hence differences in local reactivity, such as site of nucleophilicity, can be expected in **II** and **VII**. To examine further the differences between **II** and **VII**, the orbital energies and surface plots of the α-HOMO and the coefficients of the $2p_{x,y,z}$ and $3p_{x,y,z}$ basis functions forming the α-HOMO can be considered. The surface plots of the α-HOMOs of **II** and **VII** were found to be very similar (data not shown). Despite this similarity, the coefficients of the basis functions are very different in **II** and **VII** (Table 13). The α-HOMO of **VII** has contributions essentially only from the p_z orbitals, and the coefficients of these orbitals are 2–3 times greater than those for α-HOMO of **II**. Although the α-HOMO of **II** has contributions from the p_x and p_y orbitals, the net effect of these contributions leads to antibonding interactions. The orbital energies of the α-HOMOs of **II** and **VII** are −0.084 and −0.064 eV, respectively. The slightly higher value for α-HOMO of **VII** suggests that **VII** is a better nucleophile [29] than **II** (depending on the nature and energy of the LUMO of the electrophile that they interact with, e.g. molecular oxygen).

Possible roles for quinone radical and semiquinone anions

Philips and Crothers [33] have reported a correlation between transcription inhibition and dissociation rates of drug–DNA complexes while Straney and Crothers [34] have suggested a correlation between the on-rate of drug–DNA interaction and disruption of the open complex between RNA polymerase and DNA. Both these reports suggest a role for binding in the mode of action of the anthracyclines. On the other hand, Rizzo et al. [35] have reported on the kinetics of association and dissociation of calf thymus DNA and five anthracyclines including adriamycin and daunomycin. They concluded that the correlation of cytotoxicity data with both association and dissociation rates of the complexes was not significant and suggested that other factors must be involved in modulating the different biological properties of the anthracyclines. In this regard, if reactive oxygen species are responsible for the cytotoxicity, a significant correlation between binding and cytotoxicity may not be observed. Another possible explanation for the observed lack of significant correlation might be that reactive species which do not bind to the bioreceptor and/or species with only weak binding properties may be responsible for the cytotoxicity. Possible candidates as such reactive species are the $Q^{\cdot-}$ and QH^{-} forms of the drugs as opposed to $QH^{\cdot}$ and QH_2. The negatively charged $Q^{\cdot-}$ and QH^{-} can conceivably have binding properties that are different

from those that will be operative for neutral species. Moreover, geometrical changes arising from reduction activation as in the case of QH^- of **I** may lead to a different binding mechanism. AM1-SM2 [17,36]-calculated solvation free energies clearly showed that the stabilization arising from solvation of $Q^{\cdot-}$ and QH^- is substantial, and, at least in aqueous media, $Q^{\cdot-}$ and QH^- should be fairly stable and can play a considerable role in the biochemical reactivity of the drugs. The participation of reactive species such as $Q^{\cdot-}$ and QH^- in the mode of action of the drugs has not been explored before and such short-lived and reactive species may be responsible for some of the elusive nature of the mode of actions of the anthracyclines. Interestingly, the calculated electronegativities of **I** and **VI** are 6.3 and 5.94 eV, respectively, values that are comparable to that of O_2 (6.2 eV) [37]. The AM1- and PM3-calculated X_v for O_2 were 5.51 and 5.86 eV, respectively. Assuming everything else to be equal, these values suggest that **I** and **VI** can effectively compete with O_2 in a redox couple reaction. This is particularly significant, because it strongly suggests that **I** and **VI** can effectively interfere, for example, with the sequence(s) in the electron-transport chain of a mitochondrion [38]. Using the calculated values, an ordering in electronegativity can be made:

$$O_2 \sim Q > QH^{\cdot} > QH_2 > Q^{\cdot-} > QH^-$$

This suggests that $O_2/Q^{\cdot-}$ and O_2/QH^- couples are possible, leading to the formation of $O_2^{\cdot-}$ (superoxide). In light of the presumption that $O_2^{\cdot-}$ is formed by a reaction of O_2 with radical intermediates produced from anthracyclines [5,6], the redox couples shown to be feasible from the calculations are rather interesting. The calculated values also suggest that Q, $QH^{\cdot}$ and probably QH_2 can be reduced by $Q^{\cdot-}$ and QH^-, thus indicating that intermolecular and intramolecular electron transfer reactions are very feasible. Since the electronic chemical potential (μ) is the negative of X [24], the reverse of the decreasing order in absolute electronegativity will give a decreasing order in which μ reflects the decreasing order in escaping tendency of the electrons in the species. When **I** and its reduced forms are compared with **VI** and **XI**, the respective escaping tendency of the electrons in **VI** and **XI** and their reduced forms are greater.

Conclusions

A comparison of **I** and **VI** using various redox parameters, energy-partitioning analysis, enthalpies and energies for electron and proton attachments, electrostatic potentials, spin densities, etc. shows both subtle and marked differences in redox capacity and reactivity. Electron affinity and deprotonation enthalpy/energy calculations predict that the redox cycling of **VI** should be diminished provided deprotonation is the first step of the autoxidation of the reduced forms. A comparison of the AM1 and ab initio results suggests that the AM1 method can be used to establish trends in redox capacity and reactivity. The difference in the spin-density surfaces of **II** and **VII** ($Q^{\cdot-}$ forms of **I** and **VI**) is rather interesting and further similar work on two-ring (or more) model systems for the pharmacophores of the anthracycline class of anticancer agents is thought useful for the purpose of assessing differences in the reactivities of the model systems. The computationally expedient methods such as AM1 seem to be adequate to predict trends in redox capacity, nucleophilicity/electrophilicity and electron affinity. Overall, the studies seem to give some insight into the 'redox incapacitation' of 5IDN which could be explained by two factors: (i) a diminished electron affinity particularly in the first electron attachment step of the two-electron/two-proton reductive activation leading to diminished reducibility; and (ii) a greater deprotonation energy of $QH^{\cdot}$ and/or QH_2 (and may be also QH^-), leading to diminished autoxidizability. The combined effect of these factors should lead to a reduced efficiency in redox cycling. Apparently, deprotonation may play an important role in the redox cycling of the anthracyclines and further work is warranted to establish these ideas on firmer ground.

Acknowledgements

This work was supported by the HHS/MBRS Program, Grant No. S06-GM08247. This work has also benefited from the financial support for computer and software maintenance by a grant from NSF (Grant No. HRD-915407) and partial support by a Research Centers in Minority Institutions award, G12RR03062, from the Division of Research Resources, National Institutes of Health.

References

1 Lace, J.K. and Curran, C.F., In Baskin, S.I. (Ed.) Principles of Cardiac Toxicology, CRC Press, Boca Raton, FL, U.S.A., 1991, and references cited therein.
2 Halliwell, B. and Gutteridge, J.M.C., Free Radicals in Biology and Medicine, 2nd ed., Clarendon Press, Oxford, U.K., 1989, p. 327.
3 Robinson, H.H. and Kahn, S.D., J. Am. Chem. Soc., 112 (1990) 4728.
4 a. Blum, R.H. and Carter, S.K., Ann. Intern. Med., 80 (1974) 249.
b. Skougard, T. and Nissen, N.I., Dan. Med. Bull., 22 (1975) 62.
c. Carter, S.K., J. Nat. Cancer Inst., 55 (1975) 1265.
5 Arcamone, F., Doxorubicin: Anticancer Antibiotics, Academic Press, New York, NY, U.S.A., 1981.
6 a. Handa, K. and Sato, S., Gann, 66 (1975) 43.
b. Handa, K. and Sato, S., Gann, 67 (1976) 523.
c. Sato, S., Iwazumi, M. and Handa, K., Gann, 68 (1977) 603.
7 a. Boucek Jr., R.J., Olson, R.O., Brenner, D.E., Ogunbunmi, E.M., Inui, M. and Fleisher, S., J. Biol. Chem., 262 (1987) 15851.

b. Takanashi, S. and Bachur, N.R., Drug Metab. Dispos., 4 (1976) 79.
8 Angle, S.R. and Yang, W., J. Am. Chem. Soc., 112 (1990) 4524, and references cited therein.
9 Favandon, K., Biochemie, 64 (1982) 457.
10 a. Lown, J.W., Acc. Chem. Res., 15 (1982) 381.
b. Dodd, N.J.F. and Mucherjee, T., Biochem. Pharmacol., 33 (1984) 379.
c. Nohland, H. and Jordan, W., Biochem. Biophys. Res. Commun., 114 (1983) 197.
11 Myers, C.E., Muinda, J.R.F., Zweier, J. and Sinha, B.K., J. Biol. Chem., 262 (1987) 11571, and references cited therein.
12 a. Lown, J.W., Chen, H.H. and Plambeck, J.A., Biochem. Pharmacol., 28 (1979) 2563.
b. Lown, J.W., Chen, H.H. and Plambeck, J.A., Biochem. Pharmacol., 31 (1982) 575.
c. Vavies, K.J.A., Doroshow, J.H. and Hochstein, H.P., FEBS Lett., 153 (1983) 227.
d. Mimnaugh, E.G., Trush, M.A., Ciarrocchi, E.G., Lestingi, M., Fontana, M., Spadasi, S. and Montecucco, A., Biochem. J., 279 (1991) 141.
e. Nafzinger, J., Auclair, C., Florent, J.C., Guillosson, J.J. and Monneret, C., Lechemie Res., 15 (1991) 709.
f. Mimnaugh, E.G., Trush, M.A., Ginsburg, E. and Gram, T.E., Cancer Res., 42 (1982) 3574.
13 Abdella, B.R.J. and Fisher, J., Environ. Health Perspect., 64 (1985) 3.
14 Bird, D.M., Boldt, M. and Koch, T.H., J. Am. Chem. Soc., 109 (1987) 4046.
15 Dewar, M.J.S., Zoebisch, E.G., Healy, E.F. and Stewart, J.J.P., J. Am. Chem. Soc., 107 (1985) 3902. The RHF-HE method was invoked by using the key work ROHF (restricted open-shell HF) which actually defaults to the half-electron approximation. We acknowledge the comments of a reviewer for bringing this to our attention.
16 PCMODEL, Serena Software, Bloomington, IN, U.S.A., 1989.
17 AMPAC (v. 4.5), Semichem, Shawnee, KS, U.S.A., 1993.
18 Stewart, J.J.P., Quantum Chemistry Program Exchange (QCPE), No. 455, Department of Chemistry, Indiana University, Bloomington, IN, U.S.A., 1989.
19 SPARTAN (v. 3.1), Wavefunction Inc., Irvine, CA, U.S.A., 1994.
20 Frisch, M.J., Trucks, G.W., Head-Gordon, M., Gill, P.M.W., Wong, M.W., Foresman, J.B., Johnson, B.G., Schlegel, H.B., Robb, M.A., Replogle, E.S., Gomperts, R., Andres, J.L., Ragharachari, K., Binkley, J.S., Gonsalez, C., Martin, R.L., Fox, D.J., Defrees, D.J., Baker, J., Stewart, J.J.P. and Pople, J.A., GAUSSIAN92/DFT, Gaussian Inc., Pittsburgh, PA, U.S.A., 1992.
21 Koopmans, T., Physica, 1 (1934) 104.
22 Fukui, K., Acc. Chem. Res., 4 (1971) 57.
23 a. Parr, R.G., Donnelly, R.A., Levy, M. and Palke, W.E., J., Chem. Phys., 68 (1978) 3801.
b. Parr, R.G. and Pearson, R.G., J. Am. Chem. Soc., 105 (1983) 7512.
c. Pearson, R.G., Proc. Natl. Acad. Sci. USA, 83 (1980) 8440.
24 a. Brewster, M.E., Huang, M.J., Kaminski, J.J., Pop, E. and Bodor, N., J. Comput. Chem., 12 (1991) 1278.
b. Fischer, H. and Kollmar, H., Theor. Chim. Acta, 16 (1970) 163.
25 Sawyer, A., Sullivan, E. and Mariam, Y.H., J. Comput. Chem., 17 (1996) 204.
26 Eckert-Maksic', M., Bischof, P. and Maksie', Z.B., J. Mol. Struct. (THEOCHEM), 139 (1986) 179.
27 a. Bischof, P., J. Am. Chem. Soc., 98 (1976) 6844.
b. Bischof, P., Croat. Chem. Acta, 53 (1980) 51, and references cited therein.
28 a. Palumbo, M., Palu, G. and Marciani Magno, S., In Van der Goot, H., Domany, G., Pallos, L. and Timmerman, H. (Eds.) Trends in Medicinal Chemistry '88, Elsevier, New York, NY, U.S.A., 1989, p. 757.
b. Bird, D.M., Boldt, M. and Koch, T.H., J. Am. Chem. Soc., 109 (1987) 4046.
29 Isaacs, N.S., Physical Organic Chemistry, Wiley, New York, NY, U.S.A., 1987, p. 163.
30 Heinis, T., Chowdhury, S., Scott, S.L. and Kebarle, P., J. Am. Chem. Soc., 110 (1988) 400.
31 Politzer, P. and Murray, J.S., In Lipkowitz, K.B. and Boyd, D.B. (Eds.) Reviews in Computational Chemistry, VCH, New York, NY, U.S.A., 1991, Chapter 7.
32 Hehre, W.J., Practical Strategies for Electronic Structure Calculations, Wavefunction Inc., Irvine, CA, U.S.A., 1995, p. 210.
33 Phillips, D.R. and Crothers, D.M., Biochemistry, 25 (1987) 7355.
34 Straney, D.C. and Crothers, D.M., Biochemistry, 26 (1987) 1947.
35 Rizzo, V., Sacchi, N. and Menozzi, M., Biochemistry, 28 (1989) 274.
36 a. Cramer, C.J. and Truhlar, D.G., J. Comput.-Aided Mol. Design, 4 (1990) 629.
b. Cramer, C.J. and Truhlar, D.G., J. Am. Chem. Soc., 115 (1993) 8810.
37 Pearson, R.G., J. Chem. Educ., 64 (1987) 561.
38 Brey, W.S., Physical Chemistry and its Biological Application, Academic Press, New York, NY, U.S.A., 1978, p. 233.

Appendix

Energy partitioning analysis

Table 14 shows a detailed dissection of the total energies into one- and two-center terms. This table and Tables 15–17 can be used to explain why the formations of **II** from **I** and of **VIII** from **VII** are more favorable than the formations of **VII** from **VI** and of **III** from **II**, respectively. In Table 15, the differences in the total one-center terms, Δ_{21} and Δ_{54}, are −5.052 and −5.8982 eV. On this basis, one would predict that the formation of **VII** would be more favorable. However, the corresponding differences in the total two-center terms are 2.803 and 3.879 eV. The net stabilization energies will be given by the sum of the one- and two-center terms. These were calculated to be −2.248 and −2.019 eV for the formation of **II** from **I**, and **VII** from **VI**, respectively. Therefore, the greater one-center stabilization energy that favors the formation of **VII** is far outweighed by the destabilization of the two-center term in **VII** as compared to that in **II**. Furthermore, it can be seen that the primary destabilization contribution comes from the two-center neighboring pair or bonding interactions (3.03 versus 1.81 eV in

TABLE 14
DISSECTION OF ENERGIES INTO ONE- AND TWO-CENTER TERMS FOR **I–III** AND **VI–VIII**

	ΣE_A (eV)				ΣE_{AB} (eV)			
	H[b]	C[b]	O[b]	N[b]	ΣE_A (total)	N[c]	NN[d]	ΣE_{AB} (total)
1[a]	−29.216	−616.1711	−615.816		−1261.2031	−207.9532	6.7247	−201.2286
2	−30.576	−616.658	−619.028		−1266.2548	−206.1432	7.718	−198.4258
3	−36.333	−619.8087	−615.086		−1271.2277	−211.8938	6.3226	−205.5712
Δ_{21}[e]	−1.36	−0.4797	−3.212		−5.0517	1.81	0.9933	2.8034
Δ_{31}	−7.117	−3.6376	0.73		−10.0246	−3.9406	−0.4021	−4.3426
Δ_{32}	−5.757	−3.1579	3.942		−4.9729	−5.7506	−1.3954	−7.146
4[a]	−36.782	−616.8116	−308.032	−187.918	−1149.5436	−220.0414	6.984	−213.0575
5	−38.482	−617.4278	−309.581	−189.951	−1155.4418	−217.0117	7.8335	−209.1782
6	−43.688	−619.2953	−308.537	−184.892	−1156.4123	−228.6536	7.7607	−220.8929
Δ_{54}[e]	−1.7	−0.6162	−1.549	−2.033	−5.8982	3.0297	0.8495	3.8793
Δ_{64}	−6.906	−2.4837	−0.505	3.026	−6.8687	8.6122	0.7767	−7.8354
Δ_{65}	−5.206	−1.8675	1.044	−5.059	−0.9705	−11.6419	0.0728	−11.7147

[a] **1–3** and **4–6** correspond to **I–III** and **VI–VIII**, respectively (Scheme 3).
[b] Represents the sum for all atoms indicated.
[c] Represents all neighboring pair interactions.
[d] Represents all nonneighboring pair interactions.
[e] Δ values are differences between the molecule numbered first and the molecule numbered second, e.g. Δ_{21} represents the difference between the energies of **2** and **1**.

TABLE 15
CONTRIBUTIONS OF ONE- AND TWO-CENTER ENERGIES OF ELECTRON AND PROTON ATTACHMENTS (eV)

Energy terms	Electron attachment		Proton attachment	
	Δ_{21} (**I** → **II**)	Δ_{54} (**VI** → **VII**)	Δ_{32} (**II** → **III**)	Δ_{65} (**VII** → **VIII**)
(EA)[a]	−5.0517	−5.8982	−4.9729	−0.9705
(EAB)[b]	2.8034	3.8793	−7.146	−11.7147
N[c]	(1.81)	(3.03)	(−5.7506)	(−11.6419)
NN[d]	(0.99)	(0.85)	(−1.3954)	(−0.0728)
Net[e]	−2.2483	−2.0189	−12.1189	−12.6852

[a,b] Differences of [a]one- and [b]two-center terms between energies of products and reactants. The two-center contributions are the sum of neighboring (N) and nonneighboring (NN) contributions given in parentheses.
[c,d] As in Table 14.
[e] Sum of values given in rows 1 and 2.

TABLE 16
TWO-CENTER NET DESTABILIZATION ENERGIES ARISING FROM ELECTRON ATTACHMENT (eV)

Bond	**I**	**II**	Net	Bond	**VI**	**VII**	Net
O1-C2	−25.45	−22.9	2.55	O1-C2	−25.38	−22.9	2.39
C5-O5	−25.45	−22.9	2.55	C5-N6	−24.38	−20.41	3.97
Δ_{21} (EAB): 2.8034[a]				Δ_{54} (EAB): 3.8793[a]			

[a] From Table 14.

TABLE 17
TWO-CENTER NET DESTABILIZATION[a] AND/OR STABILIZATION[b] ENERGIES ARISING FROM PROTON ATTACHMENT (eV)

Bond	**II** (C5 O6)	**III** (C5 O6H)	Net[a,b]	Bond	**VII** (C5 N6H)	**VIII** (C5 N6H2)	Net[a,b]
C-O	−22.9	−16.36	6.54	C-N	−20.41	−18.44	1.97
O-H	–	−12.87	−12.87	N-H(1)	−12.78	−13.69	−0.91
				N-H(2)		−13.69	−13.69
Sum	−22.9	−29.23	−6.33		−33.19	−45.82	−12.63
			Δ_{32}: −7.146				Δ_{65}: −11.7147

[a] Positive values.
[b] Negative values.

VII and **II**, respectively). In conclusion, the reason why the formation of **II** from **I** is favored over that of **VII** from **VI** is a result of the destabilizing effect of the two-center neighboring pair interactions. A similar analysis can be made for the protonation process and the details are given in Table 15. The energy-partitioning analysis for the protonation process shows that the reason why the formation of **VIII** from **VII** is more favorable over that of **III** from **II** is a result of the stabilizing energy contribution due to the two-center neighboring pair interactions.

The partitioning of the total energy seems to indicate that the favorability or unfavorability of electron and proton attachments in **I**, **VI** and **XI** is governed by the two-center neighboring pair interactions (i.e., considering interactions between atoms within 1.9 Å of each other). The data given in Tables 1 and 2 partially reflected the reorganization of the electronic structures of benzoquinone and its analogs as they undergo reductive activation. Further insight into these structural changes can be obtained from a quantification of interatomic interactions [26] via the energy-partitioning analysis technique [27]. Figure 3 shows some selected pair interactions, from which an assessment of stabilizing (negative values) and destabilizing (positive values) effects can be determined. For bonding pair interactions, the magnitude of the energy, which is due to the contribution of the one-electron core resonance integrals to the energy of a bond, reflects the strength of the bond between the atoms of the pair [26,27]. It is evident from the data in Fig. 3 how the pair interactions change for the first two steps of Scheme 2. What is of interest is, of course, how these changes manifest themselves in the reactivity of the species resulting from the reduction. In modifying **I** to **VI**, a C5=O6 bond is replaced by C5=N6H. As a result of electron attachment to **I** and **VI**, the O1-C2 bonds in **II** and **VII** are destabilized by 2.55 and 2.39 eV, respectively, i.e. the destabilization is about the same (Table 16). The destabilization of C5-O6 in **II** and C5-N6 in **VII** is, however, 2.55 and 3.97 eV, respectively. These two values are fairly close to the total two-center energies for rows containing Δ_{21} and Δ_{54} (i.e. 2.8034 and 3.8793 eV, respectively). It has been pointed out earlier that the reason why the formation of **II** from **I** is more favorable than the formation of **VII** from **VI** is due to the greater destabilization effect of the two-center term in **VII**. From the foregoing discussion, the greater portion of this destabilization effect apparently comes from the C5-N6 pair interactions.

In going from **II** to **III** and from **VII** to **VIII**, respectively, the C5-O6 group transforms to C5-O6H and the C5-N6H group to C5-N6H2. Considering the two-center bonds in these transformations, the net stabilizations from the two transformations are −6.33 and −12.63 eV for transformations **II** to **III** and **VII** to **VIII**, respectively (Table 17). It can be noted that these values are fairly close to the two-center energies corresponding to rows Δ_{32} and Δ_{65}, respectively. The −6.33 eV value is the difference between the two-center energy of the C5-O6 bond (−22.9 eV) in **II** and the sum of the two-center energies for the C5-O6 and O6-H9 bonds (−16.36 and −12.87 eV, respectively) in **III**. The −12.63 eV value can likewise be calculated for the **VII** → **VIII** protonation process. The protonation process of **II** → **III** destabilizes the C5-O6 bond by 6.54 eV (−22.9 eV in **II** versus −16.36 eV in **III**) while that of **VII** → **VIII** destabilizes the C5-N6 bond by only 1.97 eV (−20.41 eV in **VI** versus −18.44 eV in **VIII**). There is additional stabilization in **VIII** as a result of the difference in the two-center O-H bond and N-H energies (−12.87 versus −13.69 eV). The protonation step **VII** → **VIII** also changes the N-H bond from −12.78 to −13.69 eV. The net stabilizations from protonation processes **II** → **III** and **VII** → **VIII**, −6.33 and −12.63 eV, respectively, are fairly close to the two-center neighboring pair interaction contributions of rows Δ_{32} and Δ_{65} (−7.146 and −11.7147 eV, respectively, Table 17). The reason why proton attachment is more favorable in **VII**, compared to that in **II**, can thus be explained, by and large, by the net stabilization energy involving the C-N and N-H bonds as a result of the transformation from **VII** → **VIII**. This net stabilization favors the reductive activation of **VI** to **VIII** as opposed to **I** to **III**. The reoxidation of QH$^{\cdot}$ to Q involves deprotonation and electron detachment processes. Deprotonation is less favorable in **VIII** and electron detachment is less unfavorable in **VII** (than in **III** and **II**, respectively). The energetics are, however, such that deprotonation outweighs the energetics of electron detachment and the overall reoxidation of **VIII** to **VI** is more unfavorable when compared to the reoxidation of **III** to **I**. The foregoing analysis suggests that redox cycling (reduction and autoxidation) in **VI** should be less favorable than that of I primarily due to differences in the energetics of electron attachment (to **I** and **VI**) and deprotonation (of **III** and **VIII**, i.e. the QH$^{\cdot}$ forms of **I** and **VI**, respectively) processes. Since redox cycling is presumed to play an important role in the biochemical activity of the drugs, the above findings may have a bearing on the reduced toxicity of 5IDN.